Accepted: 9 October 2018

DOI: 10.1111/jbi.13479

RESEARCH PAPER

WILEY Journal of Biogeography

Evolutionary and demographic correlates of Pleistocene coastline changes in the Sicilian wall lizard *Podarcis wagleriana*

Gabriele Senczuk[1] | D. James Harris[2] | Riccardo Castiglia[1] | Viktoria Litsi Mizan[2] | Paolo Colangelo[3] | Daniele Canestrelli[4] | Daniele Salvi[2,5]

[1]Department of Biology and Biotechnology "Charles Darwin", University of Rome "La Sapienza", Rome, Italy

[2]CIBIO-InBIO, Centro de Investigação em Biodiversidade e Recursos Genéticos, Universidade do Porto, Vairão, Portugal

[3]National Research Council, Institute of Ecosystem Study, Verbania Pallanza, Italy

[4]Department of Ecological and Biological Science, University of Tuscia, Viterbo, Italy

[5]Department of Health, Life and Environmental Sciences, University of L'Aquila, L'Aquila, Italy

Correspondence
Daniele Salvi, Department of Health, Life and Environmental Sciences, University of L'Aquila, L'Aquila, Italy.
Email: danielesalvi.bio@gmail.com

Funding information
FEDER; FCT (Fundação para a Ciência e a Tecnologia; North Portugal Regional Operational Programme; European Social Fund; Portuguese Ministério da Educação e Ciência, Grant/Award Number: IF/01627/2014; University of Rome "La Sapienza"; Programma Rita Levi Montalcini (MIUR, Ministero dell'Istruzione dell'Università e della Ricerca)

Editor: David Chapple

Abstract

Aim: Emergence of coastal lowlands during Pleistocene ice ages might have provided conditions for glacial expansions (demographic and spatial), rather than contraction, of coastal populations of temperate species. Here, we tested these predictions in the insular endemic Sicilian wall lizard *Podarcis wagleriana*.

Location: Sicily and neighbouring islands.

Methods: We sampled 179 individuals from 45 localities across the whole range of *P. wagleriana*. We investigated demographic and spatial variations through time using Bayesian coalescent models (Bayesian phylogeographic reconstruction, Extended Bayesian Skyline plots, Isolation-with-migration models) based on multilocus DNA sequence data. We used species distribution modelling to reconstruct present and past habitat suitability.

Results: We found two main lineages distributed in the east and west portions of the current species range and a third lineage restricted to a small area in the north of Sicily. Multiple lines of evidence from palaeogeographic (shorelines), palaeoclimatic (species distribution models), and multilocus genetic data (demographic and spatial Bayesian reconstructions) indicate that these lineages originated in distinct refugia, located in the north-western and south-eastern coastal lowlands, during Middle Pleistocene interglacial phases, and came into secondary contact following demographic and spatial expansions during the last glacial phase.

Main conclusions: This scenario of interglacial contraction and glacial expansion is in sharp contrast with patterns commonly observed in temperate species on the continent but parallels recent findings on other Mediterranean island endemics. Such a reverse expansion–contraction (EC) dynamic has been likely associated with glacial increases of climatically suitable coastal lowlands, suggesting this might be a general pattern in Mediterranean island species and also in other coastal regions strongly affected by glacial marine regressions during glacial episodes. This study provides explicit predictions and some methodological recommendations for testing the reverse EC model in other region and taxa.

KEYWORDS
asymmetric gene flow, glacial expansion, historical demography, Mediterranean islands, phylogeography, *Podarcis wagleriana*

1 | INTRODUCTION

Coastal settings have been cyclically reshaped during Pleistocene ice ages, when sea-level low stands caused the emergence of wide lowlands in place of shallow waters. Recent studies show that the expansion of suitable climatic conditions onto the emerged continental shelf during the Last Glacial Maximum (LGM) could have provided hospitable habitat and refugia for temperate species in many regions of the world including New Zealand, East Asia, South America, and the Mediterranean (e.g., Bisconti, Canestrelli, Colangelo, & Nascetti, 2011; Leite et al., 2016; Marske, Leschen, Barker, & Buckley, 2009; Porretta, Mastrantonio, Bellini, Somboon, & Urbanelli, 2012). Conceivably, such glaciation-induced increases in lowland habitat have had demographic, evolutionary, and biogeographical consequences on coastal populations, and in many cases could have counterbalanced the negative demographic effect of climate cooling on temperate species (Buckley, Marske, & Attanayake, 2009; Canestrelli, Cimmaruta, & Nascetti, 2007; Canestrelli & Nascetti, 2008; Leite et al., 2016; Porretta et al., 2012). The effects of Pleistocene coastline changes have been particularly prominent on island biotas. Indeed, islands have a broad expanse of coastline along which the availability of terrestrial habitats dramatically increased during glacial sea-level low stands. Newly exposed land bridges connecting islands both between them and with the continent favoured ex novo migration of species and/or intermittent secondary contacts and gene flow between populations that were isolated during interglacial stages (Fitzpatrick, Brasileiro, Haddad, & Zamudio, 2009; Hewitt, 2011a; Qi, Yuan, Comes, Sakaguchi, & Qiu, 2014). Moreover, recent studies on Mediterranean island endemics showed a close association between the demographic and spatial expansions of populations and marine regressions during the last glacial age (Bisconti et al., 2011; Salvi, Schembri, Sciberras, & Harris, 2014).

The Mediterranean Basin is a global biodiversity hotspot (Myers, Mittermeier, Mittermeier, Da Fonseca, & Kent, 2000), with a large proportion of species richness and endemism being hosted within southern peninsulas and islands (Kier et al., 2009). Recent phylogeographic studies on Mediterranean island endemics, for example on amphibian and reptiles of Western Mediterranean islands, have revealed responses to past climatic oscillations with a complexity of population structures and evolutionary histories comparable to that observed for continental species (Bisconti, Canestrelli, & Nascetti, 2013; Bisconti, Canestrelli, Salvi, & Nascetti, 2013; Ketmaier & Caccone, 2013; Ketmaier, Manganelli, Tiedemann, & Giusti, 2010; Salvi, Bisconti, & Canestrelli, 2016; Salvi, Harris, Bombi, Carretero, & Bologna, 2010; Salvi, Pinho, & Harris, 2017; Thibault, Cibois, Prodon, & Pasquet, 2016). These encompass movement of species across land bridges exposed during glacial sea-level low stands (e.g., Bisconti et al., 2011; Rodríguez et al., 2013; Salvi, Capula, Bombi, & Bologna, 2009; Salvi, Harris, Perera, Bologna, & Carretero, 2011), secondary contacts between isolated lineages within islands (Bisconti, Canestrelli, Salvi, et al., 2013; Salvi et al., 2010) as well as spatial and demographic expansion associated with glaciation-induced increase in lowland areas during marine regression (Bisconti et al., 2011; Salvi et al., 2014).

Sicily, the largest island in the Mediterranean, has contributed little to this emerging body of studies; while several features make this island and its endemics an ideal model to assess the evolutionary and demographic consequences of Pleistocene climatic oscillations on coastal and insular settings. First, Sicily experienced the highest increase in coastal plains during glacial periods among Mediterranean islands. In fact, during the LGM two wide expanses of land emerged in the southern portion and connected Sicily with the Maltese block in the south-eastern side while reducing the distance between Africa and Sicily in the south-western side with several flat-topped islands in between (Lambeck, Antonioli, Purcell, & Silenzi, 2004; Shackleton, Van Andel, & Runnels, 1984; Figure 1). Second, despite being

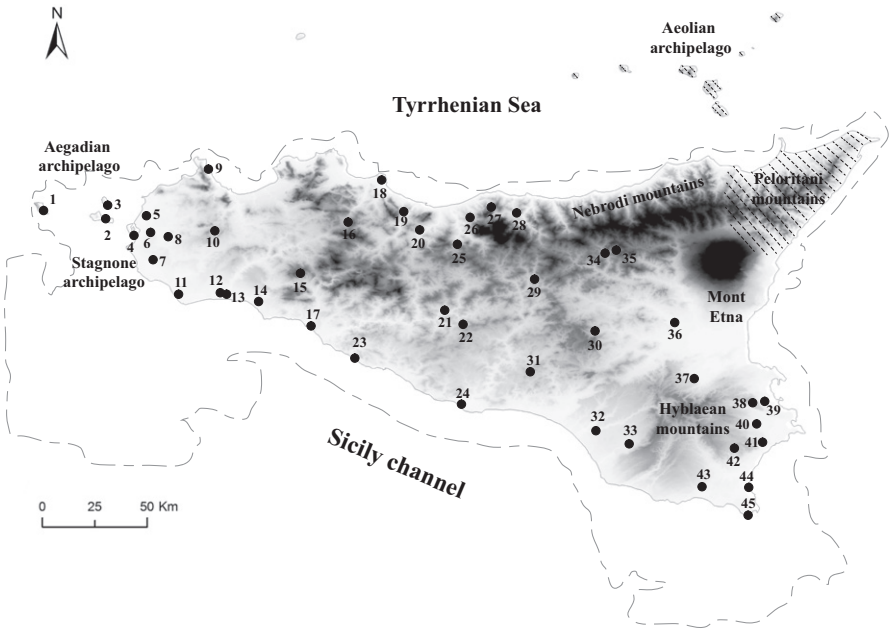

FIGURE 1 Map of the 45 sampled populations of *Podarcis wagleriana* in Sicily. Principal geographic features as mentioned in the text are indicated. The diagonal stripe pattern in the north–east portion of Sicily indicates the area which is outside of the geographic range of the species. The Aegadian archipelago includes Marettimo, Favignana, and Levanzo islands (localities 1, 2, and 3 respectively); the Stagnone archipelago includes La Scola islet (locality 4). The dashed outline represents putative coastlines during the Last Glacial Maximum (according to Lambeck et al., 2004)

characterized by a wide array of environments, Sicily displays a homogeneous physiography with the absence of substantial biogeographic discontinuities, except for Mount Etna volcano in the northwesternmost portion of the island. Finally, the southern position of Sicily in the Mediterranean Sea and the buffering action of surrounding sea have significantly reduced the effect of glacial cooling during ice ages. These features of Sicily set the scene for the glacial expansion of populations towards land bridges and lowlands made available by the sea-level regression during glacial stages, as well as for the recolonization of those portions of the island which were unsuitable during unfavourable periods.

In this study, we focused on the Sicilian wall lizard *Podarcis wagleriana*, which is endemic to the Sicily Island (Western Mediterranean; see Figure 1). Unlike many other Sicilian endemics, which colonized the island in recent times (Late Pleistocene) from the Italian peninsula (e.g., Bezerra et al., 2016; Canestrelli & Nascetti, 2008; Fritz et al., 2005), *P. wagleriana* is palaeoendemic on the island (Harris, Pinho, Carretero, Corti, & Böhme, 2005). Furthermore, life-history and ecological features of *P. wagleriana* are relatively well known (Capula, 2006; Turrisi & Vaccaro, 1998). This species has a marked preference for low-altitude grasslands, below 600 m. a.s.l., thus providing an ideal case to investigate long-term demographic and evolutionary consequences of Pleistocene climate changes in coastal areas. Here, we reconstructed the demographic and range variations and habitat suitability through time to evaluate whether the pattern of genetic variation observed in the Sicilian wall lizard reflects (a) a glacial expansion of populations in coastal lowland emerged during sea-level regressions (Bisconti et al., 2011; Salvi et al., 2014), or (b) a "classic" Expansion–Contraction (EC) model of size and range contraction to refugia during glacials, followed by post-glacial population growth and range expansion (Hewitt, 1996, 2004; Provan & Bennet, 2008; Schmitt, 2007). Under the first scenario, we expect (a) genetic signatures of demographic and spatial expansion of populations during the last glacial phase (starting from 115–120 thousands year ago, ka), associated with a (b) significant increase of climatically suitable habitat along newly emerged coastal lowlands, and (c) the location of the ancestral populations of current lineage(s) to be inferred in the proximity of these coastal plains. Alternatively, if *P. wagleriana* conforms the predictions of the EC model we expect (a) a signal of demographic and range expansion of the species during post-glacial phases, with (b) an estimated coalescent time of intraspecific genetic diversity dating back to a glacial phase, and (c) ancestral area(s) of current lineage(s) and past habitat suitability not necessarily located in coastal regions.

2 | MATERIALS AND METHODS

2.1 | Sampling and laboratory procedures

We collected 179 individuals of *P. wagleriana* from 45 localities in Sicily and the Aegadian and Stagnone archipelagos. Sampling covered the entire species range distribution and included the two recognized subspecies, that is, the nominal subspecies and *P. w. marettimensis* endemic to Marettimo island (Figure 1). Geographical coordinates and sample size for each sampled locality are given in Table 1. Tail tips were collected from sampled individuals and stored in 96% ethanol. Animals were then released at the capture location.

Genomic DNA was extracted from stored tissues following the extraction protocol of Salah and Martinez (1997) with incubation at 56°C with proteinase K and DNA precipitation with isopropanol. We amplified and sequenced two mitochondrial DNA (mtDNA) gene fragments, the NADH dehydrogenase subunit 4 with flanking tRNAs (*nd4*) and the cytochrome-b (*cytb*), and two nuclear (nuDNA) gene fragments, the Melanocortin receptor 1 (*mc1r*) and the β-fibrinogen intron 7 (β-*fibint7*). The specific PCR primers for each gene fragment are reported in (Supporting information Appendix S1: Table S1.1). PCR products were purified and sequenced by Macrogen Inc. (www.macrogen.com).

2.2 | Data analysis

We used GENEIOUS 4.5 (http://www.geneious.com, Kearse et al., 2012) to check electropherograms, call heterozygote positions, build consensus sequences, and perform multiple sequence alignments. Mitochondrial sequences of *nd4* and *cytb* were concatenated (mtDNA dataset).

The gametic phase of nuclear sequences was resolved using the Bayesian algorithm implemented in PHASE 2.1 (Stephens & Donnelly, 2003; Stephens, Smith, & Donnelly, 2001). Prior to PHASE analyses, we resolved manually insertion-deletion (indel) polymorphisms of the β-*fibint7* fragment in 56 individuals and used the resolved haplotypes as known phases in subsequent PHASE runs. We conducted three independent runs for each gene with the initial 1,000 iterations discarded as burn-in, 1 as thinning interval, and 1,000 post-burn-in iterations. We estimated the number of haplotypes (n), as well as nucleotide (π) and haplotype (h) diversity for each locus using DNASP 5.1 (Librado & Rozas, 2009). The most appropriate model of sequence evolution for each dataset was selected in JMODELTEST (Posada, 2008), using the Akaike information criterion (*cytb* + *nd4*: HKY; β-*fibint7*: HKY + G; *mc1r*: HKY + I + G).

Gene genealogies for both mitochondrial and nuclear markers were reconstructed as phylogenetic networks using the statistical parsimony approach (Templeton, Crandall, & Sing, 1992) under the 95% probability connection limit, employing the software TCS 1.21 (Clement, Posada, & Crandall, 2000).

The time to the most recent common ancestor (TMCRA) of the main mtDNA lineages was inferred by estimating a time-calibrated Bayesian phylogeny in BEAST 1.8.1 (Drummond, Suchard, Xie, & Rambaut, 2012). In the absence of fossil data useful to calibrate the tree, we used the substitution rate previously estimated by Salvi et al. (2014) for the *nd4* gene fragment of Sicilian *Podarcis* (including *P. wagleriana*). We ran the analysis using a strict clock model with a lognormal distribution prior (μ = 0.0115, σ = 0.14) for the *nd4* (Salvi et al., 2014), and a large uninformative prior for the *cytb* substitution rate (uniform distribution: 0, 0.25). The coalescent Bayesian skyline

TABLE 1 Sampling localities with their code, province (in brackets) and geographic coordinates; sample size at each location and the frequencies (in brackets) of each mitochondrial and nuclear haplotype is reported

				mtDNA		*mc1r*		β-*fibint7*	
Locality		Lat.	Long.	*n*	Haplotype(s)	*n*	Haplotype(s)	*n*	Haplotype(s)
1	Marettimo (TP)	37,9712	12,0696	21	H1(1), H2(1), H3(7), H4(2), H5(2), H6(2), H7(3), H8(1) H9(1), H10(1)	42	M1(13), M2(10), M3(1), M4(2), M5(4), M6(5), M7(1), M8(2), M9(1), M10(2), M11(1)	36	F1(6), F2(2), F3(2), F4(1), F5 (7), F6(3), F7(3), F8(2), F9(1), F10(2), F11(1), F12(1), F13 (1), F14(1), F15(1), F16(1), F17(1)
2	Favignana (TP)	37,9152	12,3195	13	H12(3), H13(1), H14 (2), H15(1), H16(2), H17(1), H18(1), H28 (2)	26	M1(1), M4(8), M5(2), M8(3), M10(2), M12 (4), M13(1), M14(2), M15(2), M15(1)	22	F1(4), F6(11), F18(1), F19(1), F20(1), F21(2), F22(1), F23 (1)
3	Levanzo (TP)	37,9922	12,3381	6	H19(4), H20(1), H28(1)	12	M1(4), M6(2), M8(3), M12(1), M17(1), M18 (1)	12	F1(2), F6(7), F18(2), F24(1)
4	La Scola (TP)	37,8629	12,4568	9	H11(3), H28(6)	22	M12(2), M19(20)	10	F6(1), F7(4), F25(2), F26(1), F27(1), F28(1)
5	Palma (TP)	37,9528	12,4998	4	H22(1), H28(3)	8	M1(1), M4(1), M6(1), M8(2), M12(1), M20 (1), M21(1)	8	F1(2), F5(1), F7(1), F18(2), F28(1), F29(1)
6	Granatello (TP)	37,8835	12,5282	5	H23(1), H24(1), H28(3)	6	M4(1), M8(2), M10(1), M12(1), M19(1)	6	F6(1), F30(1), F31(1), F32(1), F33(1), F34(1)
7	Ciavolo (TP)	37,7815	12,5546	1	H28(1)	2	M6(1),M15(1)	2	F26(1), F35(1)
8	Ponte di Cuddia (TP)	37,8722	12,6039	3	H25(1), H26(1), H28(1)	6	M4(2), M6(1), M16(1), M20(2)	4	F22(1), F32(1), F36(1), F37(1)
9	Zingaro (TP)	38,0877	12,7972	8	H21(1), H27(1), H28 (5), H29(1)	16	M4(3), M5(1), M6(3), M8(7), M15(1), M19 (1)	16	F5(1), F6(3), F7(1), F15(1), F18(4), F38(1), F39(1), F40 (1), F41(1), F42(1), F43(1)
10	Vita (Tr)	37,8915	12,8012	1	H30(1)	2	M4(1), M5(1)	2	F7(1), F15(1)
11	Lago della Priola (TP)	37,6095	12,6484	4	H28(2), H31(1), H32(1)	8	M4(2), M5(1), M6(3), M8(1), M12(1)	8	F1(1), F6(1), F18(3), F44(3)
12	Santa Teresa (TP)	37,6200	12,8305	5	H28(2), H33(2), H34(1)	10	M4(3), M8(2), M15(3), M22(1), M23(1)	8	F6(3), F15(1), F18(3), F45(1)
13	Selinunte (TP)	37,6166	12,841	5	H28(3), H35(1), H36(1)	8	M4(1), M5(3), M6(1), M8(1), M12(1), M15 (1)	6	F5(1), F6(1), F7(1), F38(1), F46(4), F47(1)
14	Menfi (AG)	37,5903	12,993	2	H28(1), H32(1)	4	M4(2), M8(1), M12(1)	4	F6(1), F7(1), F15(1), F47(1)
15	Contessa Entellina (PA)	37,7093	13,1739	1	H37(1)	2	M4(1), M6(1)	2	F1(1), F7(1)
16	Lago dello Scanzano (PA)	37,4799	13,2211	6	H28(4), 40(1), H42(1)	12	M4(7), M5(3), M12(1), M15(1)	10	F5(1), F6(2), F18(1), F26(1), F27(1), F47(1), F48(1), F49 (1), F59(1)
17	Ribera (AG)	38,105	12,677	5	H38(1), H39(1), H44 (1), H45(2)	12	M4(2), M6(1), M8(4), M12(1), M15(3), M22 (1)	10	F1(2), F6(1), F20(1), F27(1), F41(1), F44(1), F51(1), F52 (1), F53(1)
18	Aspra (PA)	38,1072	13,5143	5	H40(4), H43(1)	10	M4(4), M5(1), M6(1), M8(2), M23(2)	8	F1(1), F6(1), F10(1), F18(2), F20(1), F35(1), F54(1)
19	Contrada Speciale (PA)	37,9766	13,6108	3	H40(3)	6	M4(1), M8(2), M23(2), M24(1)	2	F7(1), F55(1)
20	Caccamo (PA)	37,897	13,6779	2	H41(1), H48(1)	4	M4(4)	4	F15(1), F56(1), F57(1), F58(1)
21	Mussomeli (CL)	37,5365	13,7894	4	H46(1), H49(1), H50 (1), H65(1)	8	M4(4), M15(4)	6	F18(4), F47(1), F59(1)
22	Montedoro (CL)	37,4468	13,8477	1	H46(1)	4	M4(2), M15(2)	\	\
23	Siculiana Marina (AG)	37,3404	13,3921	2	H46(2)	6	M4(2), M8(1), M15(1), M25(1), M26(1)	2	F18(1), F60(1)

(Continues)

TABLE 1 (Continued)

				mtDNA		*mc1r*		β-*fibint7*	
Locality		Lat.	Long.	*n*	Haplotype(s)	*n*	Haplotype(s)	*n*	Haplotype(s)
24	Torre di Gaffe (AG)	37,1504	13,8561	5	H51(1), H52(1), H53 (2), H54(1)	10	M4(7), M6(1), M15(2)	8	F1(1), F5(1), F18(2), F61(1), F62(1), F63(1), F64(1)
25	Sclafani Bagni (PA)	37,8386	13,846	2	H55(1), H56(1)	4	M4(1), M6(1), M15(2)	2	F18(1), F65(1)
26	Collesano (PA)	37,9455	13,8977	2	H48(1), H57(1)	4	M4(2), M15(2)	2	F18(2)
27	Gibilmanna (PA)	37,986	13,986	1	H57(1)	2	M4(1), M15(1)	\	\
28	Castelbuono (PA)	37,9608	14,1040	3	H48(1), H57(2)	6	M4(5), M15(1)	6	F5(1), F18(3), F66(1), F67(1)
29	Alimena (PA)	37,6781	14,1712	2	H53(2)	4	M4(2), M8(1), M15(1)	2	F18(1), F59(1)
30	Aidone (EN)	37,4619	14,4413	4	H53(1), H58(1), H59(2)	8	M4(1), M15(7)	8	F5(1), F18(1), F59(1), F61(1), F68(1), F69(1), F70(1), F70 (1)
31	Mazzarino (CL)	37,2901	14,1501	5	H46(2), H53(1), H60 (1), H61(1)	10	M4(4), M15(6)	8	F5(2), F18(3), F64(1), F72(1), F73(1)
32	Acate (RG)	37,0313	14,4512	4	H47(1), H62(1), H63 (1), H64(1)	8	M4(3), M15(4), M27(1)	8	F1(1), F18(2), F47(1), F61(1), F73(2), F74(1)
33	Vittoria (RG)	36,9673	14,5503	3	H64(2), H66(1)	6	M4(1), M5(1), M8(1), M15(1), M20(2)	2	F75(1), F76(1)
34	Cerami (EN)	37,8197	14,5274	2	H53(1), H67(1)	4	M4(3), M15(1)	4	F5(2), F18(1), F77(1)
35	Capizzi (ME)	37,809	14,4752	1	H66(1)	2	M4(1), M20(1)	2	F78(1), F79(1)
36	Sferro (CT)	37,4885	14,7728	2	H69(1), H70(1)	4	M4(1), M5(1), M8(1), M15(1)	4	F18(1), F67(1), F80(1), F81(1)
37	Francofonte (SR)	37,2630	14,8646	5	H53(2), H59(1), H71 (1), H72(1)	6	M4(2), M15(3), M28(1)	8	F59(2), F61(1), F62(1), F73 (1), F82(1), F83(1), F84(1)
38	Melilli (SR)	37,1603	15,0947	2	H73(1), H74(1)	4	M15(4)	4	F18(1), F61(2), F67(1)
39	Contrada Talà (SR)	37,1598	15,1592	1	H74(1)	2	M4(1), M15(1)	2	F85(1), F86(1)
40	Floridia (SR)	37,0635	15,121	2	H53(1), H74(1)	4	M4(1), M5(1), M27(1), M29(1)	2	F32(1), F81(1)
41	Cassibile (SR)	36,9826	15,1637	3	H75(1), H76(1), H77(1)	6	M4(2), M15(3), M30(1)	2	F87(2)
42	Pietà San Giovannello (SR)	36,9599	15,0339	3	H78(1), H79(1), H80(1)	10	M4(1), M8(1), M15(5), M27(3)	6	F18(1), F61(2), F88(1), F89 (1), F90(1)
43	Ispica (RG)	36,7947	14,8817	3	H73(1), H81(2)	6	M5(1), M8(2), M15(2), M31(1)	6	F18(2), F32(1), F59(1), F61 (1), F91(1)
44	Vendicari (SR)	36,7869	15,0935	1	H82(1)	2	M5(1), M8(1)	2	F18(1), F92(1)
45	Portopalo di Capopassero (SR)	36,6681	15,0996	6	H81(1), H83(4), H84(1)	12	M5(3), M8(2), M15(7)	10	F18(3), F73(2), F93(3), F94 (1), F95(1)

model was used as tree prior, as it imposes minimal assumptions on the data (Drummond, Ho, Rawlence, & Rambaut, 2007). BEAST was run for 100 million generations sampling parameters each 10,000 generations. Here and for all subsequent analyses with BEAST, the software TRACER 1.6 (Rambaut, Suchard, Xie, & Drummond, 2014) was used to check for proper mixing and convergence among runs. Trees from a stationary distribution (burn-in = 25%) were used to calculate an annotated Maximum Clade Credibility tree in TreeAnnotator 1.7.5 (Drummond et al., 2012).

In order to assess whether divergence between the main mtDNA lineages occurred with or without nuclear gene flow, we fitted an isolation-with-migration model (Hey & Nielsen, 2004) to the nuDNA data, using previous phylogenetic inferences to define population groups. Several preliminary runs were performed using the software IMA2 (Hey, 2010a, 2010b), in order to identify appropriate upper bound scalars that encompassed the posterior distribution of each parameter (-t10, -q15, -m4). The final IMa2 analysis was performed in M-mode with HKY models applied to both *mc1r* and β-*fibint7*, using five independent Markov-coupled chains with a geometric heating scheme (-ha0.96, -hb0.8). A total of 100,000 genealogies were retained following burn-in. The run stationarity was assessed by checking for low autocorrelation of splitting time terms, high swap rates between chains and inspecting no trend in the splitting time plots (Hey, 2010a). To assess whether estimates of migration rates (m0 and m1) between the two main lineages were significantly different from zero or from each other, we run IMa2 in L-mode, and used the genealogies sampled in M-mode to estimate joint posterior distribution of nested models with different migration scenarios. We

compared through likelihood ratio (LLR) tests the fully parameterized model with four simpler migration scenarios: bidirectional migration, unidirectional migration in one direction or in the other, and zero migration.

We investigated the demographic and spatial components of *P. wagleriana* range variations through time, using Bayesian coalescent models implemented in BEAST. We analysed each main phylogenetic group supported by the previous analyses separately, in order to avoid the potential biases generated by population structure (Heller, Chikhi, & Siegismund, 2013). Historical demographic changes were inferred for each group based on mtDNA and nuDNA data through Extended Bayesian Skyline Plot (EBSP) analyses (Drummond et al., 2012; Heled & Drummond, 2008). Tree models of the mtDNA fragments were linked, whereas substitution and clock models were unlinked across all genes. The *nd4* rate prior was set as in previous BEAST analyses, and used as a reference to guide rate estimates for the other gene fragments. EBSP analyses were run for 300 million generations sampling every 30,000 steps. Graphical representations of the effective population size through time were generated following Heled (2010).

Spatial diffusion processes out of the ancestral areas were estimated by means of Bayesian phylogeographic (BP) reconstructions in continuous space (Lemey, Rambaut, Welch, & Suchard, 2010). This analysis was run for each marker separately, and results were then compared to identify major areas of convergence. After several preliminary runs aimed at fine-tuning the analysis parameters for each dataset (mtDNA, β-*fibint7*, and the *mc1r*), we carried out final runs using a relaxed random walk diffusion model with Cauchy distribution (Lemey et al., 2010). For the nuclear markers, we used substitution rates derived from previous EBSP estimations. In order to reduce computational burden and help the analyses to converge, we used a strict molecular clock model for all markers analysed, and the Bayesian skyline as a coalescent tree prior. MCMCs were run for 200 million generations sampled every 20,000 generations. The ancestral areas and the spatial diffusion processes out of these areas were then visualized using SPREAD v. 1.0.5 (Bielejec, Rambaut, Suchard, & Lemey, 2011).

2.3 | Species distribution modelling

We used species distribution models (SDM) to reconstruct present and past habitat suitability distributions of *P. wagleriana* and assess whether the divergence between mitochondrial haplogroups is associated with allopatry in distinct areas separated by low habitat suitability during the LGM (*c.* 21 ka) and Last Interglacial (LIG; *c.* 120–140 ka). Species occurrence records were collected mainly during fieldwork with a few records derived from Global Biodiversity Information Facility (GBIF, http://www.gbif.org/). The obtained dataset includes 138 occurrence coordinates, which covers the entire range of the species thoroughly (bearing in mind its reduced insular extent). To avoid duplicate coordinates within the same cell, the complete dataset was subsampled to the spatial resolution of the environmental layers used (0.5 arc min, *c.* 1 km), resulting in 90 occurrence records.

The SDM was created using the bioclimatic variables available from the WorldClim database (Hijmans, Cameron, Parra, Jones, & Jarvis, 2005). These variables are often highly autocorrelated. To avoid a bias due to the introduction of many variables with a high level of correlation, we choose nine bioclimatic variables that we deemed as biologically meaningful based on our knowledge of the ecology of the species and that were not highly autocorrelated (Pearson correlation coefficient $r < 0.75$): mean diurnal Range (BIO2), Isothermality (BIO3 = BIO2/BIO7 × 100), temperature seasonality (BIO4), minimum temperature of the coldest month (BIO6), temperature annual range (BIO7), mean temperature of the driest quarter (BIO9), annual precipitation (BIO12), precipitation seasonality (BIO15), and precipitation of the warmest quarter (BIO18).

The current habitat suitability for *P. wagleriana* was generated using an ensemble forecasting as implemented in the R package 'biomod2' (Thuiller, Lafourcade, Engler, & Araújo, 2009). We used four different algorithms that estimate species distribution using environmental predictors together with species occurrences: Maxent (Phillips, Anderson, & Schapire, 2006; Phillips & Dudík, 2008), Gradient Boosting Machines (Ridgeway, 1999), Generalized Linear Model (McCullagh & Nelder, 1989), and General Additive Model (Hastie & Tibshirani, 1990). These algorithms were used to predict the species occurrence under current, LGM and LIG conditions. To validate the model, 70% of the localities were used to train the model and 30% were used to test it (Thuiller et al., 2009). This procedure was replicated 10 times. For each occurrence dataset, we used 10,000 background points of the distribution area of *P. wagleriana* to characterize the climate of the study area and to represent pseudo-absences. The predictive capability of the obtained models was assessed with the AUC (Hanley & McNeil, 1982) and with the true skill statistic TSS (Allouche, Tsoar, & Kadmon, 2006). Successively, a final ensemble model was obtained considering only those models with AUC >0.7 and TSS >0.4. Finally, the obtained model for the present-day was projected to the LGM condition, using both the Community Climate System Model (CCSM) and the Model for Interdisciplinary Research on Climate (MIROC), and to the LIG condition (Otto-Bliesner, Marshall, Overpeck, Miller, & Hu, 2006) available in the WorldClim database.

3 | RESULTS

We obtained a concatenated mtDNA alignment of 1,453 base pairs (bp) in length (*nd4*: 611 bp; *cytb*: 842 bp) for 178 individuals from 45 populations. The nucDNA dataset consisted of 286 phased sequences of β-*fibint7* (576 bp) and 360 sequences of *mc1r* (583 bp). The mtDNA dataset included 84 unique haplotypes defined by 98 polymorphic sites; the β-*fibint7* dataset showed 95 haplotypes with 48 polymorphic sites and the *mc1r* dataset 31 haplotypes with 21 polymorphic sites (see Supporting Information Appendix S1: Table S1.2 for GenBank accession numbers).

The mitochondrial genealogy inferred by the statistical parsimony approach returned a single network with three main haplogroups

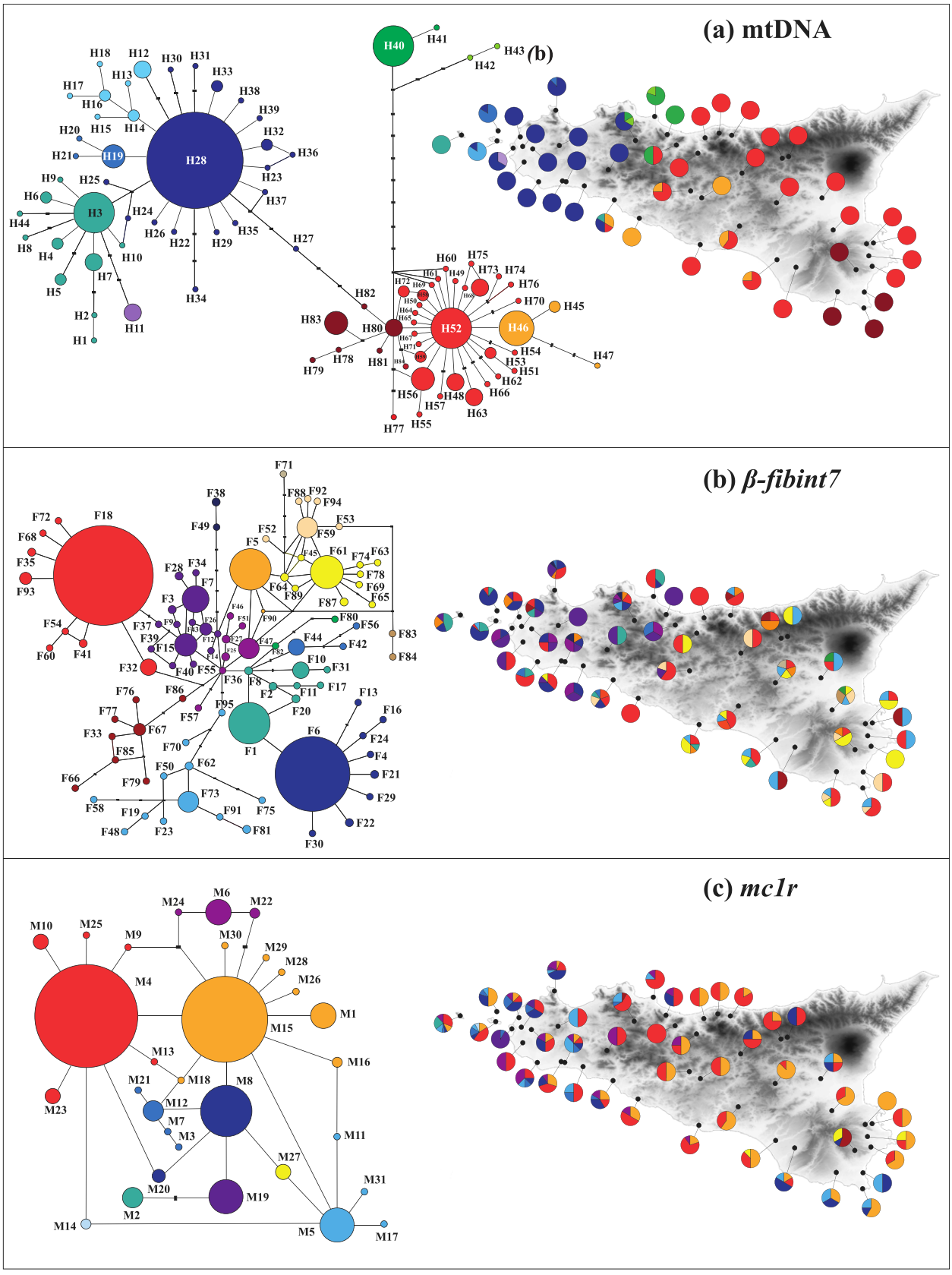

FIGURE 2 Phylogenetic networks showing the relationships between the mtDNA (a), β-*fibint7* (b), and *mc1r* (c) haplotypes of *Podarcis wagleriana* and their geographic distribution in Sicily. Circle size is proportional to the haplotype frequency; small black rectangles represent one substitution. Pie charts in the maps represent the haplotype frequency at each sampling locality

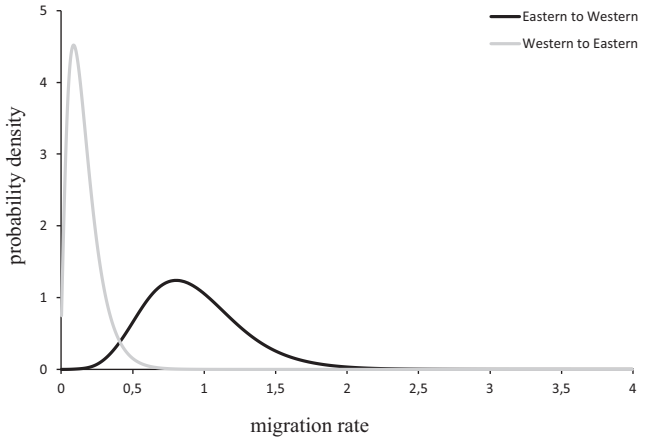

FIGURE 3 Marginal posterior densities estimates for migration rates between the Eastern and Western lineages of *Podarcis wagleriana* based on the isolation-with-migration model

showing a clear geographic association (Figure 2a). One haplogroup clusters haplotypes sampled in the western portion of the species range (Western lineage), a second group is defined by haplotypes carried by individuals from the eastern part of the range (Eastern lineage), and a third haplogroup includes haplotypes from a restricted area in the northern region (North Lineage). Both the Western and the Eastern lineage subnetworks showed a star-like shape. Overall, the three mitochondrial lineages show a parapatric pattern of distribution with three localities of co-occurrence (samples 16, 17, and 20) placed in areas of contiguity between lineages.

Within the Western Lineage, populations from the Egadi Islands (Marettimo, Favignana, Levanzo) and from La Scola islet carry a high proportion of private mtDNA haplotypes (H1-21 and H44), which form distinct clusters in the network relative to haplotypes found in western continental Sicily. Within the Eastern Lineage, haplotypes from the Hyblean region in SE Sicily (H78-H83) and from the central portion of Sicily (H45-H47) show some differentiation from the most common haplogroup widespread in the eastern species' range and which shows a star-like shape (H52 and derived haplotypes).

Unlike the mtDNA, the nuDNA genealogies did not show a clear phylogeographic structure. For both nuclear loci, the most common haplotypes (F18, M4, and M15, with allele frequencies of 16%, 25%, and 20% respectively) are distributed throughout the species range (Figure 2b,c). Geographic association was weak also in low frequency haplotypes, although at the β-*fibint7* locus a moderate geographic association is apparent with haplotypes sampled either in the western or in the eastern portions of the species range clustering together.

The TMRCA of *P. wagleriana* was estimated to have occurred at 350 ka (95% HPD interval: 570–180 ka), while the split time between the Eastern and the Western lineage was estimated at 190 ka (95% HPD interval: 320–100 ka) (see Supporting Information Appendix S2: Figure S2).

Estimates of nuclear gene flow between populations belonging to distinct mitochondrial lineages showed asymmetric migration

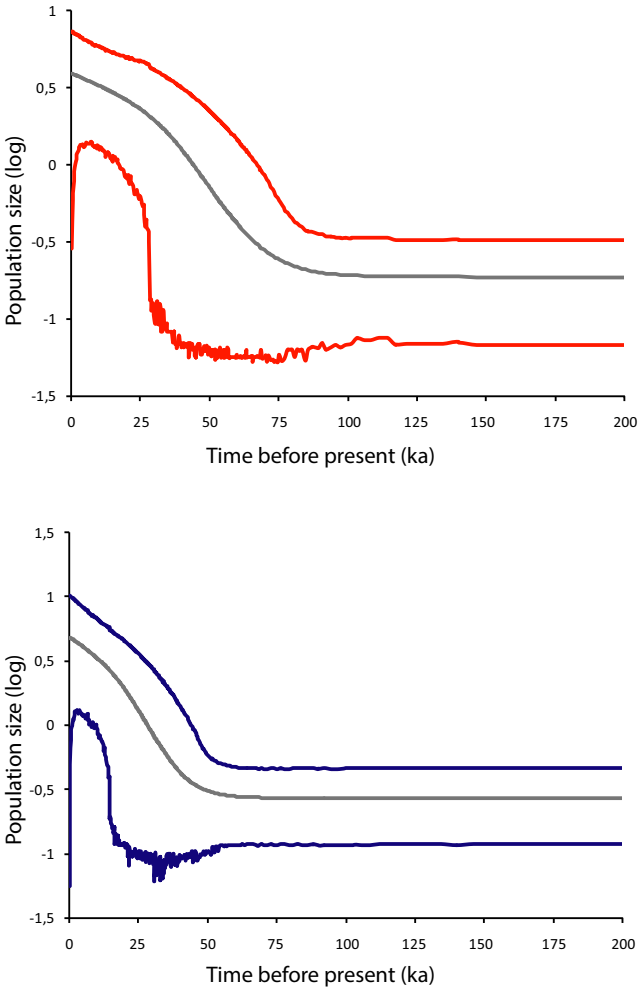

FIGURE 4 Extended Bayesian skyline plots representing the historical demographic trends of the Eastern lineage (red) and the Western lineage (blue) of *Podarcis wagleriana*. Grey lines are median estimates, while coloured lines represent confidence intervals

rates. In particular, posterior densities for migration rate parameters indicate greater gene flow from the Eastern (m1 = 0.9) into the Western (m2 = 0.09) range than in the opposite direction (Figure 3). This is also supported by the LLR tests on the four nested models: the model with a migration parameter from East to West was the best nested model (LLR = 2.05) while models with zero-migration rates as well as those with equal migration rates between groups were rejected.

The EBSP showed historical demographic trends with a marked population expansion for both the Western and the Eastern lineages, starting at *c.* 45 and 65 ka respectively (Figure 4). Inspection of the number of demographic functions for each time interval of the EBSPs indicates that the demographic inferences can be deemed as reliable backward in time until *c.* 200 ka for both lineages.

The BP reconstruction of the spatial diffusion process carried out on the mtDNA dataset suggested that ancestral area for the Western lineage was located in a small area including the westernmost coast of Sicily and the Favignana Island (Figure 5a). From this area,

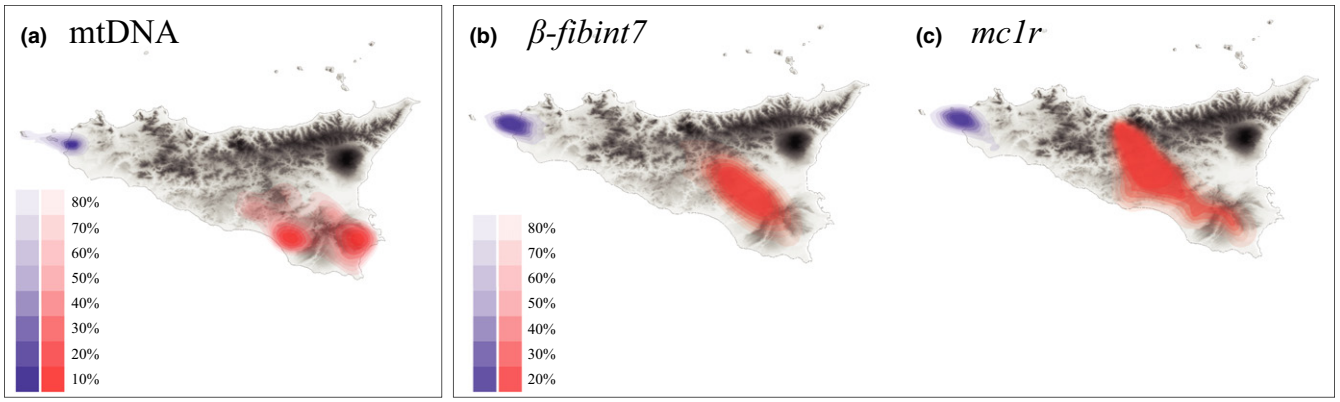

FIGURE 5 Highest posterior density (HPD) regions of the geographical location of the most recent common ancestor of the main lineages of *Podarcis wagleriana* based on mtDNA (a), β-*fibint7* (b), and *mc1r* (c)

the western lineage expanded eastward during the last glacial phase, reaching the current zone of secondary contact with the Eastern lineage at the end of this phase or during the early post-glacial phase (Supporting Information Appendix S3). This BP reconstruction was remarkably concordant with those generated based on both the *bfib* and the *mc1r* nuclear loci (Figure 5b,c and Supporting Information Appendix S3). The ancestral area estimated for the Eastern lineage based on mtDNA data was located in the south-eastern portion of Sicily, and its westward expansion was inferred to have occurred earlier within the last glacial phase reaching the current zone of secondary contact with the Western lineage at the end of this phase (Figure 5a and Supporting Information Appendix S3). BP inferences based on nuclear gene fragments showed large uncertainty regarding the location of the ancestral area of the Eastern lineage, but still includes the easternmost portion in both loci (Figure 5b,c).

3.1 | Species distribution modelling

The SDMs for the Sicilian wall lizard built using nine bioclimatic variables have high values of AUC and TSS (mean AUC >0.9 and mean TSS >0.7 for all the models). The four models reported very similar habitat suitability predictions.

The present-day habitat suitability reconstruction showed high suitability along coastal areas and moderate habitat suitability in central regions. Specifically, three main areas of high suitability scores have been identified: (a) the Hyblaean coastal areas, (b) lowlands located within the eastern portion and (c) along restricted areas of the northern coast (Figure 6a). It is noteworthy that very low habitat suitability is associated with the north-east portion of the island corresponding to Nebrodi and Peloritani mountain ranges, where the species is considered absent (Sindaco, 2006). The habitat suitability at the LGM shows similar patterns between the two projections obtained using MIROC or CCSM palaeoclimatic models. On the whole, models predict an increase of suitable areas during the LGM for *P. wagleriana*, as much as ten times compared to current models of habitat suitability. During the LGM, Sicily showed the highest suitability scores in southern lowland coastal areas made available by the glacial marine regression. Also in the northern coastal regions, high suitability is limited to coastal lowlands that emerged during the LGM sea-level low stand. However, the extent of these northern lowlands was reduced except for the area where populations belonging to the North lineage are currently located (Figure 6b). With respect to the present-day conditions, score projections during LIG showed a much lower habitat suitability especially for central regions, while moderate suitability was limited to coastal lowlands (Figure 6c).

4 | DISCUSSION

Pleistocene climatic oscillations have influenced range dynamics of temperate species, either by displacing their bioclimatic optima, or by affecting the geography of physical habitat availability (Hewitt, 1996, 2000, 2004; Schmitt, 2007; Taberlet, Fumagalli, Wust-Saucy, & Cosson, 1998). Our analyses show that these processes have tightly interacted to shape current patterns of genetic variation among *P. wagleriana* populations.

Palaeo-coastline data and SDM analyses indicate that the amount of bioclimatically suitable areas available to *P. wagleriana* was substantially higher during the last glacial period compared to the interglacials, LIG and current (Lambeck et al., 2004; Figures 1 and 6). During the glacial maximum, favourable conditions for this species were mediated both by the extension of coastal lowlands during sea-level regressions and by the high suitability of these newly emerged lands (Figure 6a). A remarkably different scenario is instead apparent for the preceding interglacial stage which was characterized by a dramatic decrease of climatic suitability, especially in the inland portion of Sicily, as well as by a significant reduction of lowland areas associated with shorelines during a sea-level high stand (Figure 6c). These contrasting patterns of potential area of distribution and climatic suitability between interglacial and glacial stages provide a spatial and demographic scenario for *P. wagleriana* with interglacial contraction and fragmentation and glacial expansion and (secondary) connection.

Coalescent reconstructions of time and location of the MRCA of intraspecific lineages show a clear association between the

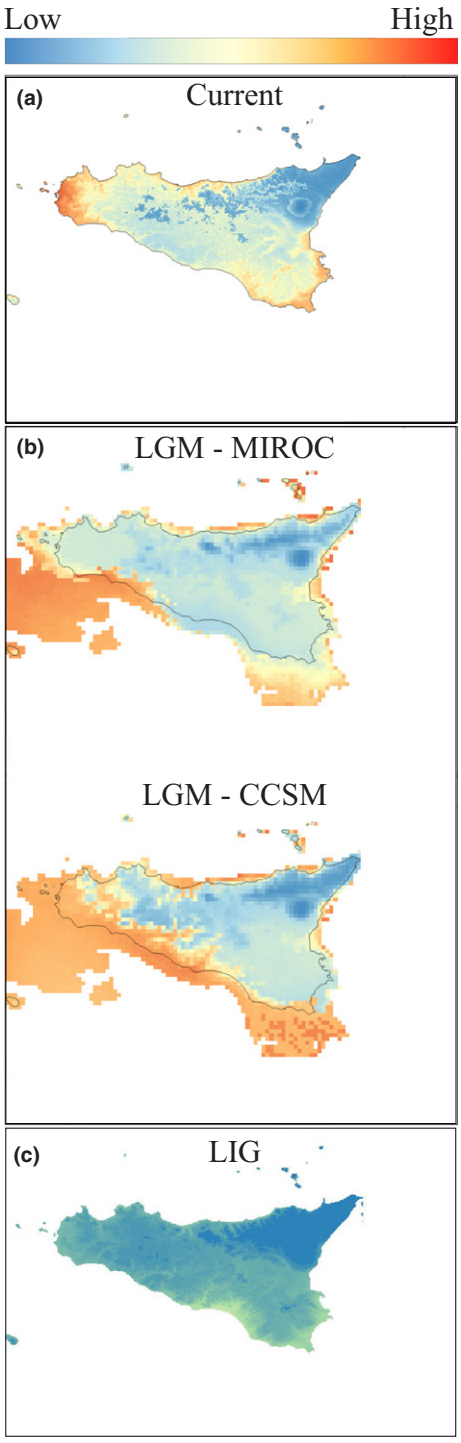

FIGURE 6 Species distribution models (SDMs) for *Podarcis wagleriana* under the current (a), the LGM (based on MIROC and CCSM circulation models) (b) and the LIG (c) conditions

phylogeographic structure of *P. wagleriana* and habitat fragmentation during the LIG periods. TMRCAs estimates show that the divergence between the main mitochondrial lineages had preceded the last glacial period, being placed at the end of the Middle Pleistocene, likely within the LIG for the split between the Western and Eastern lineages or even before for the divergence of the Northern lineage (see Supporting Information Appendix S2: Figure S2). According to the Bayesian phylogeographical reconstructions, the ancestral populations of the Western and the Eastern lineages have been located in the north-western and south-eastern coastal lowlands, respectively (Figure 5). These areas most likely acted as independent (interglacial) refugia, allowing persistence as well as allopatric differentiation of *P. wagleriana* populations.

During the subsequent glacial phase, habitat availability reached the optimum for *P. wagleriana*, just in the proximity of these ancestral areas (Figure 6b). The historical demographic reconstructions show that changes in population size of both lineages followed the glacial increase in the amount of habitat available. Indeed, both the Western and the Eastern lineage underwent a sudden demographic expansion during the same time that large coastal lowlands with favourable climate conditions became available in the western and south-eastern portion of the palaeo-Sicily (Figures 4 and 6). Such a glacial scenario is made particularly robust by the convergence of multiple line of evidence from independent palaeogeographic (shorelines) palaeoclimatic (SDM) and multilocus genetic data (EBSP).

According to the Bayesian phylogeographical analysis, a spatial diffusion process towards the central portion of the island took place during the last glacial period, leading to a secondary contact between lineages well before the onset of the LGM (Supporting Information Appendix S3). Genetic imprints of this secondary contact are evident at both the mitochondrial and nuclear genomes, albeit they are clearer in the former (Figure 2). Instances of co-occurrence of eastern and western mtDNA lineages are in fact restricted to areas located at the lineages' range boundaries, within our samples 16, 17, and 20 (Figure 2a). Instead, a weaker differentiation is apparent along the east–west axis at the nuclear loci (Figure 2b,c), and a secondary contact zone is hardly discernible. A shallower phylogeographic pattern at nuclear compared to mitochondrial loci is, however, not surprising especially for recent divergences (Avise, 2000; Hare, 2001; Hudson, 1990; Moore, 1995; Pamilo & Nei, 1988). It has been frequently explained as the result of differences in effective populations sizes and substitution rates between mitochondrial and nuclear genomes (for examples on *Podarcis* lizard see Pinho, Harris, & Ferrand, 2008; Salvi, Harris, Kaliontzopoulou, Carretero, & Pinho, 2013; Salvi et al., 2014), or as the result of male-biased gene flow (Toews & Brelsford, 2012). These processes are in fact not mutually exclusive and might have both contributed to the weak phylogeographic pattern observed at nuclear loci in *P. wagleriana*. On the other hand, a significant contribution of nuclear gene flow to this pattern is indicated by the Isolation-with-Migration analyses. Indeed, the estimated posterior densities for migration rate parameters show a peak at values greater than zero (Figure 3), and models with zero-migration rates were statistically rejected by LLR tests. Interestingly, migration rate parameters indicate greater gene flow from the eastern range into the western range than in the opposite direction (Figure 3), suggesting asymmetric patterns of gene-exchange between lineages.

Strong evidence for asymmetric nuclear introgression between intraspecific lineages, following secondary contact, has been recently provided for the common wall lizard *Podarcis muralis* (While et al.,

2015; Yang et al., 2018). In this species, strong asymmetries in male competitive ability and mating success between lineages originated in distinct glacial refugia explains the pattern of asymmetric hybridization upon secondary contact, with the replacement of nuclear characters of the subdominant lineage (While et al., 2015). Recent studies have described a general model of spatial sorting underlying the selection of (male) traits of competitive ability and mating success during sudden spatial expansions (Phillips, Brown, & Shine, 2010; Shine et al., 2011). The evolutionary consequences of such changes when two divergent lineages come into secondary contact is a hot topic of research (Canestrelli, Bisconti, & Carere, 2016; Canestrelli, Porretta, et al., 2016; Lowe & McPeek, 2014). Since much of the complexities that are inherent to continental settings might be attenuated within an insular context (Warren et al., 2015), whether the insular endemic Sicilian wall lizard *P. wagleriana* represents an additional case of such evolutionary processes, arises as an intriguing question for further studies.

5 | FINAL REMARKS

In most temperate species studied to date, range-wide patterns of genetic variation have been explained by geographic and demographic EC dynamics, driven by Pleistocene climatic oscillations (Hewitt, 1996, 2000, 2004; Hickerson et al., 2010; Provan & Bennet, 2008; Schmitt, 2007; Taberlet et al., 1998). In these species, contraction phases were associated to unfavourable glacial climates, while expansion phases to more suitable interglacial conditions. Instead, the evolutionary history of *P. wagleriana* does not conform to this scenario. Our results indicated that this species underwent a contraction phase during the LIG, and an expansion phase during the last glacial period, following what can be called a "reverse EC" dynamic. Interestingly, this pattern parallels similar findings for the Maltese wall lizard *Podarcis filfolensis* (Salvi et al., 2014), endemic to the Maltese Archipelago, and for the Tyrrhenian tree frog *Hyla sarda*, endemic to Corsica and Sardinia islands (Bisconti et al., 2011). Even in these thermophilic species, demographic and range expansions have been associated to glacial increases of climatically suitable coastal lowlands, suggesting that a reverse EC dynamic might be a general, albeit still underappreciated, pattern in Mediterranean island species.

The applicability of the reverse EC model might well extend beyond the Mediterranean region, in all those geographic settings where the glaciation-induced increase of coastal lowlands was significant, and the climatic conditions were suitable for the colonization of these emerged lands. For example, in New Zealand during the LGM the land surface area was more than double the current one and evidence of coastal refugia have been found in studies on stick insects (Buckley, Marske, & Attanayake, 2010; Buckley et al., 2009) and beetles (Marske et al., 2009). The majority of suitable habitat for these species during the LGM was predicted in coastal areas that are currently submerged, and in the case of *Argosarchus horridus* a demographic expansion phase was apparent during the last glacial period (Buckley et al., 2009). Likewise, a study on the tiger mosquito in the temperate regions of Southeast Asia also highlighted the positive role of the glacial-induced emergence of lowlands in maintaining populations of increased size during glacial phases (Porretta et al., 2012).

The integration of phylogeographic, historical demographic, SDM approaches and palaeoshorelines reconstructions proved to be particularly fruitful for the documentation of the reverse EC model (Bisconti et al., 2011; Salvi et al., 2014; this study) and its possible application outside the Mediterranean region as discussed above. Patterns conform to the reverse EC model are likely easier to identify on islands than on the continent (but see Canestrelli et al., 2007; Canestrelli & Nascetti, 2008; Senczuk, Colangelo, De Simone, Aloise, & Castiglia, 2017). Indeed, the increase of terrestrial habitats during glacial sea-level low stands has been proportionally larger for island endemics compared to wide-ranging continental species (Lambeck et al., 2004; Thiede, 1978), leaving a marked expansion imprint on historical spatial and demographic patterns on island species. Moreover, sampling efforts in phylogeographic surveys of island endemics are typically denser along coastal lowlands with respect to studies of continental species, given the smaller spatial scale of analysis and the high proportion of coastal habitat on islands. Therefore, whether the combination of phylogeographic and past habitat suitability analyses with denser sampling schemes for coastal populations of continental species might reveal reverse EC patterns in other regions and taxa, is a relevant question that deserves future research effort.

ACKNOWLEDGEMENTS

We thank Antigoni Kaliontzopoulou and Joana Mendes for the help in sample collection and Maurizio Sarà, Enrico Bellia, and Mario Lo Valvo for the access to the collection of the Museum of Zoology, University of Palermo. Special thanks are addressed to Dario D'Eustacchio, who tragically passed away during his PhD, for his precious suggestions and for his valuable help in the field. Lizards were captured and handled under permits from the Italian Ministry of Environment (PNM-2012-0009747, PNM-2012-00017879, MATTM 46783). This work was partially supported by: FEDER through the COMPETE program, Portuguese national funds through the FCT (Fundação para a Ciência e a Tecnologia, Portugal); the project "Genomics and Evolutionary Biology" cofinanced by North Portugal Regional Operational Programme 2007/2013 (ON.2–O Novo Norte), under the National Strategic Reference Framework (NSRF-ERDF). D.J.H. is supported by FCT, funds from the European Social Fund and Portuguese Ministério da Educação e Ciência (contract IF/01627/2014). R.C. is supported by "Progetti di Ricerca" funds, University of Rome "La Sapienza". D.S. is supported by the program 'Rita Levi Montalcini' (MIUR, Ministero dell'Istruzione dell'Università e della Ricerca) for the recruitment of young researchers at the University of L'Aquila.

DATA ACCESSIBILITY

DNA sequences: GenBank accession numbers for each individual can be found in Supporting Information Appendix S1.

ORCID

Gabriele Senczuk http://orcid.org/0000-0001-8889-2290
D. James Harris http://orcid.org/0000-0001-5144-2421
Paolo Colangelo http://orcid.org/0000-0002-0283-3618
Daniele Salvi http://orcid.org/0000-0002-3804-2690

REFERENCES

Allouche, O., Tsoar, A., & Kadmon, R. (2006). Assessing the accuracy of species distribution models: Prevalence, kappa and the true skill statistic (TSS). *Journal of Applied Ecology*, *43*, 1223–1232. https://doi.org/10.1111/j.1365-2664.2006.01214.x

Avise, J. C. (2000). *Phylogeography: The history and formation of species*. Cambridge, MA: Harvard University Press.

Bezerra, A. M., Annesi, F., Aloise, G., Amori, G., Giustini, L., & Castiglia, R. (2016). Integrative taxonomy of the Italian pine voles, *Microtus savii* group (Cricetidae, Arvicolinae). *Zoologica Scripta*, *45*, 225–236. https://doi.org/10.1111/zsc.12155

Bielejec, F., Rambaut, A., Suchard, M. A., & Lemey, P. (2011). SPREAD: Spatial phylogenetic reconstruction of evolutionary dynamics. *Bioinformatics*, *27*, 2910–2912. https://doi.org/10.1093/bioinformatics/btr481

Bisconti, R., Canestrelli, D., Colangelo, P., & Nascetti, G. (2011). Multiple lines of evidence for demographic and range expansion of a temperate species (*Hyla sarda*) during the last glaciation. *Molecular Ecology*, *20*, 5313–5327. https://doi.org/10.1111/j.1365-294X.2011.05363.x

Bisconti, R., Canestrelli, D., & Nascetti, G. (2013). Has living on islands been so simple? Insights from the insular endemic frog *Discoglossus montalentii*. *PLoS ONE*, *8*, e55735. https://doi.org/10.1371/journal.pone.0055735

Bisconti, R., Canestrelli, D., Salvi, D., & Nascetti, G. (2013). A geographic mosaic of evolutionary lineages within the insular endemic newt *Euproctus montanus*. *Molecular Ecology*, *22*, 143–156. https://doi.org/10.1111/mec.12085

Buckley, T. R., Marske, K. A., & Attanayake, D. (2009). Identifying glacial refugia in a geographic parthenogen using palaeoclimate modelling and phylogeography: The New Zealand stick insect *Argosarchus horridus* (White). *Molecular Ecology*, *18*, 4650–4663. https://doi.org/10.1111/j.1365-294X.2009.04396.x

Buckley, T. R., Marske, K., & Attanayake, D. (2010). Phylogeography and ecological niche modelling of the New Zealand stick insect *Clitarchus hookeri* (White) support survival in multiple coastal refugia. *Journal of Biogeography*, *37*, 682–695. https://doi.org/10.1111/j.1365-2699.2009.02239.x

Canestrelli, D., Bisconti, R., & Carere, C. (2016). Bolder takes all? The behavioral dimension of biogeography. *Trends in Ecology & Evolution*, *31*, 35–43. https://doi.org/10.1016/j.tree.2015.11.004

Canestrelli, D., Cimmaruta, R., & Nascetti, G. (2007). Phylogeography and historical demography of the Italian treefrog *Hyla intermedia* reveals multiple refugia, population expansions and secondary contacts within peninsular Italy. *Molecular Ecology*, *16*, 4808–4821. https://doi.org/10.1111/j.1365-294X.2007.03534.x

Canestrelli, D., & Nascetti, G. (2008). Phylogeography of the pool frog *Rana* (*Pelophylax*) *lessonae* in the Italian peninsula and Sicily: Multiple refugia, glacial expansions and nuclear-mitochondrial discordance. *Journal of Biogeography*, *35*, 1923–1936. https://doi.org/10.1111/j.1365-2699.2008.01946.x

Canestrelli, D., Porretta, D., Lowe, W. H., Bisconti, R., Carere, C., & Nascetti, G. (2016). The tangled evolutionary legacies of range expansion and hybridization. *Trends in Ecology & Evolution*, *31*, 677–688. https://doi.org/10.1016/j.tree.2016.06.010

Capula, M. (2006). Sicilian wall lizard *Podarcis wagleriana* Gistel, 1868. *Atlante degli Anfibi e dei Rettili d'Italia [Atlas of Italian amphibians and reptiles]*. In R. Sindaco, D. Giuliano, E. Razzetti & F. Bernini (pp. 494–497). Edizioni Polistampa, Firenze: Societas Herpetologica Italica.

Clement, M., Posada, D., & Crandall, K. A. (2000). TCS: A computer program to estimate gene genealogies. *Molecular Ecology*, *9*, 1657–1659. https://doi.org/10.1046/j.1365-294x.2000.01020.x

Drummond, A. J., Ho, S. Y., Rawlence, N., & Rambaut, A. (2007). A rough guide to BEAST 1.4.

Drummond, A. J., Suchard, M. A., Xie, D., & Rambaut, A. (2012). Bayesian phylogenetics with BEAUti and the BEAST 1.7. *Molecular Biology and Evolution*, *29*, 1969–1973. https://doi.org/10.1093/molbev/mss075

Fitzpatrick, S. W., Brasileiro, C. A., Haddad, C. F., & Zamudio, K. R. (2009). Geographical variation in genetic structure of an Atlantic Coastal Forest frog reveals regional differences in habitat stability. *Molecular Ecology*, *18*, 2877–2896. https://doi.org/10.1111/j.1365-294X.2009.04245.x

Fritz, U., Fattizzo, T., Guicking, D., Tripepi, S., Pennisi, M. G., Lenk, P., & Wink, M. (2005). A new cryptic species of pond turtle from southern Italy, the hottest spot in the range of the genus *Emys* (Reptilia, Testudines, Emydidae). *Zoologica Scripta*, *34*, 351–371. https://doi.org/10.1111/j.1463-6409.2005.00188.x

Hanley, J. A., & McNeil, B. J. (1982). The meaning and use of the area under a receiver operating characteristic (ROC) curve. *Radiology*, *143*, 29–36. https://doi.org/10.1148/radiology.143.1.7063747

Hare, M. P. (2001). Prospects for nuclear gene phylogeography. *Trends in Ecology and Evolution*, *16*, 700–706. https://doi.org/10.1016/S0169-5347(01)02326-6

Harris, D. J., Pinho, C., Carretero, M. A., Corti, C., & Böhme, W. (2005). Determination of genetic diversity within the insular lizard *Podarcis tiliguerta* using mtDNA sequence data, with a reassessment of the phylogeny of *Podarcis*. *Amphibia-Reptilia*, *26*, 401–407. https://doi.org/10.1163/156853805774408676

Hastie, T. J., & Tibshirani, R. J. (1990). *Generalized additive models (vol. 43)*. Boca Raton, FL: CRC Press.

Heled, J. (2010). Extended Bayesian skyline plot tutorial. Retrieved from http://beast-mcmc.googlecode.com/svn-history/r3936/trunk/doc/tutorial/EBSP/ebsp-tut.pdf

Heled, J., & Drummond, A. J. (2008). Bayesian inference of population size history from multiple loci. *BMC Evolutionary Biology*, *8*, 289. https://doi.org/10.1186/1471-2148-8-289

Heller, R., Chikhi, L., & Siegismund, H. R. (2013). The confounding effect of population structure on Bayesian skyline plot inferences of demographic history. *PLoS ONE*, *8*, e62992. https://doi.org/10.1371/journal.pone.0062992

Hewitt, G. M. (1996). Some genetic consequences of ice ages and their role in divergence and speciation. *Biological Journal of the Linnean Society*, *58*, 247–276. https://doi.org/10.1111/j.1095-8312.1996.tb01434.x

Hewitt, G. M. (2000). The genetic legacy of the Quaternary ice ages. *Nature*, *405*, 907–913. https://doi.org/10.1038/35016000

Hewitt, G. M. (2004). Genetic consequences of climatic oscillations in the Quaternary. *Philosophical Transactions of the Royal Society of London B: Biological Sciences*, *359*, 183–195. https://doi.org/10.1098/rstb.2003.1388

Hewitt, G. M. (2011a). Quaternary phylogeography: The roots of hybrid zones. *Genetica*, *139*, 617–638. https://doi.org/10.1007/s10709-011-9547-3

Hey, J. (2010a). Isolation with migration models for more than two populations. *Molecular Biology and Evolution*, *27*, 905–920. https://doi.org/10.1093/molbev/msp296

Hey, J. (2010b). The divergence of chimpanzee species and subspecies as revealed in multipopulation isolation-with-migration analyses. *Molecular Biology and Evolution*, *27*, 921–933. https://doi.org/10.1093/molbev/msp298

Hey, J., & Nielsen, R. (2004). Multilocus methods for estimating population sizes, migration rates and divergence time, with applications

to the divergence of *Drosophila pseudoobscura* and *D. persimilis*. *Genetics*, *167*, 747–760. https://doi.org/10.1534/genetics.103.024182

Hickerson, M. J., Carstens, B. C., Cavender-Bares, J., Crandall, K. A., Graham, C. H., Johnson, J. B., … Yoder, A. D. (2010). Phylogeography's past, present, and future: 10 years after Avise, 2000. *Molecular Phylogenetics and Evolution*, *54*, 291–301. https://doi.org/10.1016/j.ympev.2009.09.016

Hijmans, R. J., Cameron, S. E., Parra, J. L., Jones, P. G., & Jarvis, A. (2005). Very high resolution interpolated climate surfaces for global land areas. *International Journal of Climatology*, *25*, 1965–1978. https://doi.org/10.1002/(ISSN)1097-0088

Hudson, R. R. (1990). Gene geneaologies and the coalescent process. *Oxford Survey in Evolutionary Biology*, *7*, 1–44.

Kearse, M., Moir, R., Wilson, A., Stones-Havas, S., Cheung, M., Sturrock, S., & Thierer, T. (2012). Geneious Basic: An integrated and extendable desktop software platform for the organization and analysis of sequence data. *Bioinformatics*, *28*, 1647–1649. https://doi.org/10.1093/bioinformatics/bts199

Ketmaier, V., & Caccone, A. (2013). Twenty years of molecular biogeography in the West Mediterranean islands of Corsica and Sardinia: Lessons learnt and future prospects. In *Current progress in biological research* (Chapter 4, pp. 71–93). Rijeka, Croatia: InTech.

Ketmaier, V., Manganelli, G., Tiedemann, R., & Giusti, F. (2010). Peri-Tyrrhenian phylogeography in the land snail *Solatopupa guidoni* (Pulmonata). *Malacologia*, *52*, 81–96. https://doi.org/10.4002/040.052.0106

Kier, G., Kreft, H., Lee, T. M., Jetz, W., Ibisch, P. L., Nowicki, C., & Barthlott, W. (2009). A global assessment of endemism and species richness across island and mainland regions. *Proceedings of the National Academy of Sciences of the United States of America*, *106*, 9322–9327. https://doi.org/10.1073/pnas.0810306106

Lambeck, K., Antonioli, F., Purcell, A., & Silenzi, S. (2004). Sea-level change along the Italian coast for the past 10,000yr. *Quaternary Science Reviews*, *23*, 1567–1598. https://doi.org/10.1016/j.quascirev.2004.02.009

Leite, Y. L., Costa, L. P., Loss, A. C., Rocha, R. G., Batalha-Filho, H., Bastos, A. C., … Pardini, R. (2016). Neotropical forest expansion during the last glacial period challenges refuge hypothesis. *Proceedings of the National Academy of Sciences of the United States of America*, *113*, 1008–1013. https://doi.org/10.1073/pnas.1513062113

Lemey, P., Rambaut, A., Welch, J. J., & Suchard, M. A. (2010). Phylogeography takes a relaxed random walk in continuous space and time. *Molecular Biology and Evolution*, *27*, 1877–1885. https://doi.org/10.1093/molbev/msq067

Librado, P., & Rozas, J. (2009). DnaSP v5: A software for comprehensive analysis of DNA polymorphism data. *Bioinformatics*, *25*, 1451–1452. https://doi.org/10.1093/bioinformatics/btp187

Lowe, W. H., & McPeek, M. A. (2014). Is dispersal neutral? *Trends in Ecology & Evolution*, *29*, 444–450. https://doi.org/10.1016/j.tree.2014.05.009

Marske, K. A., Leschen, R. A., Barker, G. M., & Buckley, T. R. (2009). Phylogeography and ecological niche modelling implicate coastal refugia and trans-alpine dispersal of a New Zealand fungus beetle. *Molecular Ecology*, *18*, 5126–5142. https://doi.org/10.1111/j.1365-294X.2009.04418.x

McCullagh, P., & Nelder, J. A. (1989). *Generalized linear models*. Boca Raton, FL: Chapman and Hall/CRC. https://doi.org/10.1007/978-1-4899-3242-6

Moore, W. S. (1995). Inferring phylogenies from mtdna variation: Mitochondrial-gene trees versus nuclear-gene trees. *Evolution*, *49*, 718–726.

Myers, N., Mittermeier, R. A., Mittermeier, C. G., Da Fonseca, G. A., & Kent, J. (2000). Biodiversity hotspots for conservation priorities. *Nature*, *403*, 853. https://doi.org/10.1038/35002501

Otto-Bliesner, B. L., Marshall, S. J., Overpeck, J. T., Miller, G. H., & Hu, A. (2006). Simulating Arctic climate warmth and icefield retreat in the last interglaciation. *Science*, *311*, 1751–1753. https://doi.org/10.1126/science.1120808

Pamilo, P., & Nei, M. (1988). Relationships between gene trees and the species trees. *Molecular Biology and Evolution*, *5*, 568–583.

Phillips, S. J., Anderson, R. P., & Schapire, R. E. (2006). Maximum entropy modeling of species geographic distributions. *Ecological Modelling*, *190*, 231–259. https://doi.org/10.1016/j.ecolmodel.2005.03.026

Phillips, B. L., Brown, G. P., & Shine, R. (2010). Life-history evolution in range-shifting populations. *Ecology*, *91*(6), 1617–1627. https://doi.org/10.1890/09-0910.1

Phillips, S. J., & Dudík, M. (2008). Modeling of species distributions with Maxent: New extensions and a comprehensive evaluation. *Ecography*, *31*, 161–175. https://doi.org/10.1111/j.0906-7590.2008.5203.x

Pinho, C., Harris, D. J., & Ferrand, N. (2008). Non-equilibrium estimates of gene flow inferred from nuclear genealogies suggest that Iberian and North African wall lizards are an assemblage of incipient species. *BMC Evolutionary Biology*, *8*, 63. https://doi.org/10.1186/1471-2148-8-63

Porretta, D., Mastrantonio, V., Bellini, R., Somboon, P., & Urbanelli, S. (2012). Glacial history of a modern invader: Phylogeography and species distribution modelling of the Asian tiger mosquito *Aedes albopictus*. *PLoS ONE*, *7*, e44515. https://doi.org/10.1371/journal.pone.0044515

Posada, D. (2008). jModelTest: Phylogenetic model averaging. *Molecular Biology and Evolution*, *25*, 1253–1256. https://doi.org/10.1093/molbev/msn083

Provan, J., & Bennet, K. D. (2008). Phylogeographic insights into cryptic glacial refugia. *Trend in Ecology and Evolution*, *23*, 564–571. https://doi.org/10.1016/j.tree.2008.06.010

Qi, X. S., Yuan, N., Comes, H. P., Sakaguchi, S., & Qiu, Y. X. (2014). A strong 'filter'effect of the East China Sea land bridge for East Asia's temperate plant species: Inferences from molecular phylogeography and ecological niche modelling of *Platycrater arguta* (Hydrangeaceae). *BMC Evolutionary Biology*, *14*, 41. https://doi.org/10.1186/1471-2148-14-41

Rambaut, A., Suchard, M., Xie, D., & Drummond, A.(2014). Tracer v1. 6. Retrieved from http://beast.bio.ed.ac.uk.Tracer (Online May 29, 2015).

Ridgeway, G. (1999). The state of boosting. *Computing Science and Statistics*, *31*, 172–181.

Rodríguez, V., Brown, R. P., Terrasa, B., Pérez-Mellado, V., Castro, J. A., Picornell, A., & Ramon, M. M. (2013). Multilocus genetic diversity and historical biogeography of the endemic wall lizard from Ibiza and Formentera, *Podarcis pityusensis* (Squamata: Lacertidae). *Molecular Ecology*, *22*, 4829–4841. https://doi.org/10.1111/mec.12443

Salah, M. A., & Martinez, I. (1997). Universal and rapid salt-extraction of high quality genomic DNA for PCR-based techniques. *Nucleic Acid Research*, *25*, 4692–4693.

Salvi, D., Bisconti, R., & Canestrelli, D. (2016). High phylogeographical complexity within Mediterranean islands: Insights from the Corsican fire salamander. *Journal of Biogeography*, *43*, 192–203. https://doi.org/10.1111/jbi.12624

Salvi, D., Capula, M., Bombi, P., & Bologna, M. A. (2009). Genetic variation and its evolutionary implications in a Mediterranean island endemic lizard. *Biological Journal of the Linnean Society*, *98*, 661–676. https://doi.org/10.1111/j.1095-8312.2009.01313.x

Salvi, D., Harris, D. J., Bombi, P., Carretero, M. A., & Bologna, M. A. (2010). Mitochondrial phylogeography of the Bedriaga's rock lizard, *Archaeolacerta bedriagae* (Reptilia: Lacertidae) endemic to Corsica and Sardinia. *Molecular Phylogenetics and Evolution*, *56*, 690–697. https://doi.org/10.1016/j.ympev.2010.03.017

Salvi, D., Harris, D. J., Kaliontzopoulou, A., Carretero, M. A., & Pinho, C. (2013). Persistence across Pleistocene ice ages in Mediterranean and extra-Mediterranean refugia: Phylogeographic insights from the common wall lizard. *BMC Evolutionary Biology*, *13*, 147. https://doi.org/10.1186/1471-2148-13-147

Salvi, D., Harris, D. J., Perera, A., Bologna, M. A., & Carretero, M. A. (2011). Preliminary survey on genetic variation within the

pygmy algyroides, *Algyroides fitzingeri*, across Corsica and Sardinia. *Amphibia-Reptilia*, *32*, 281–286. https://doi.org/10.1163/017353711X556989

Salvi, D., Pinho, C., & Harris, D. J. (2017). Digging up the roots of an insular hotspot of genetic diversity: Decoupled mito-nuclear histories in the evolution of the Corsican-Sardinian endemic lizard *Podarcis tiliguerta*. *BMC Evolutionary Biology*, *17*, 63. https://doi.org/10.1186/s12862-017-0899-x

Salvi, D., Schembri, P. J., Sciberras, A., & Harris, D. J. (2014). Evolutionary history of the Maltese wall lizard *Podarcis filfolensis*: Insights on the 'Expansion–Contraction' model of Pleistocene biogeography. *Molecular Ecology*, *23*, 1167–1187. https://doi.org/10.1111/mec.12668

Schmitt, T. (2007). Molecular biogeography of Europe: Pleistocene cycles and postglacial trends. *Frontiers in Zoology*, *4*, 11. https://doi.org/10.1186/1742-9994-4-11

Senczuk, G., Colangelo, P., De Simone, E., Aloise, G., & Castiglia, R. (2017). A combination of long term fragmentation and glacial persistence drove the evolutionary history of the Italian wall lizard *Podarcis siculus*. *BMC Evolutionary Biology*, *17*, 6. https://doi.org/10.1186/s12862-016-0847-1

Shackleton, J. C., Van Andel, T. H., & Runnels, C. N. (1984). Coastal paleogeography of the central and western Mediterranean during the last 125,000 years and its archaeological implications. *Journal of Field Archaeology*, *11*, 307–314.

Shine, R., Brown, G. P., & Phillips, B. L. (2011). An evolutionary process that assembles phenotypes through space rather than through time. *Proceedings of the National Academy of Sciences of the United States of America*, *108*, 5708–5711. https://doi.org/10.1073/pnas.1018989108

Sindaco, R. (2006). *Atlante degli Anfibi e dei Rettili d'Italia*. Firenze, Italy: Societas Herpetologica Italica, Edizioni Polistampa.

Stephens, M., & Donnelly, P. (2003). A comparison of Bayesian methods for haplotype reconstruction from population genotype data. *The American Journal of Human Genetics*, *73*, 1162–1169. https://doi.org/10.1086/379378

Stephens, M., Smith, N. J., & Donnelly, P. (2001). A new statistical method for haplotype reconstruction from population data. *The American Journal of Human Genetics*, *68*, 978–989. https://doi.org/10.1086/319501

Taberlet, P., Fumagalli, L. A., Wust-Saucy, A. G., & Cosson, J. F. (1998). Comparative phylogeography and postglacial colonization routes in Europe. *Molecular Ecology*, *7*, 453–464. https://doi.org/10.1046/j.1365-294x.1998.00289.x

Templeton, A. R., Crandall, K. A., & Sing, C. F. (1992). A cladistic analysis of phenotypic associations with haplotypes inferred from restriction endonuclease mapping and DNA sequence data. III. Cladogram estimation. *Genetics*, *132*, 619–633.

Thibault, J. C., Cibois, A., Prodon, R., & Pasquet, E. (2016). Quaternary history of an endemic passerine bird on Corsica Island: Glacial refugium and impact of recent forest regression. *Quaternary Research*, *85*, 271–278. https://doi.org/10.1016/j.yqres.2016.01.002

Thiede, J. (1978). A glacial Mediterranean. *Nature*, *276*, 680–683. https://doi.org/10.1038/276680a0

Thuiller, W., Lafourcade, B., Engler, R., & Araújo, M. B. (2009). BIOMOD–a platform for ensemble forecasting of species distributions. *Ecography*, *32*, 369–373. https://doi.org/10.1111/j.1600-0587.2008.05742.x

Toews, D. P., & Brelsford, A. (2012). The biogeography of mitochondrial and nuclear discordance in animals. *Molecular Ecology*, *21*, 3907–3930. https://doi.org/10.1111/j.1365-294X.2012.05664.x

Turrisi, G. F., & Vaccaro, A. (1998). Contributo alla conoscenza degli Anfibi e dei Rettili di Sicilia. *Bollettino delle sedute della Accademia Gioenia di Scienze Naturali in Catania*, *30*, 5–88.

Warren, B. H., Simberloff, D., Ricklefs, R. E., Aguilée, R., Condamine, F. L., Gravel, D., … Thébaud, C. (2015). Islands as model systems in ecology and evolution: Prospects fifty years after MacArthur-Wilson. *Ecology Letters*, *18*, 200–217. https://doi.org/10.1111/ele.12398

While, G. M., Michaelides, S., Heathcote, R. J., MacGregor, H. E., Zajac, N., Beninde, J., … Uller, T. (2015). Sexual selection drives asymmetric introgression in wall lizards. *Ecology Letters*, *18*, 1366–1375. https://doi.org/10.1111/ele.12531

Yang, W., While, G. M., Laakkonen, H., Sacchi, R., Zuffi, M. A., Scali, S., … Uller, T. (2018). Genomic evidence for asymmetric introgression by sexual selection in the common wall lizard. *Molecular Ecology*, *27*, 4213–4224. https://doi.org/10.1111/mec.14861

BIOSKETCH

Gabriele Senczuk is interested in evolutionary processes driving biodiversity patterns and on islands biogeography, using phylogeographic and molecular population genetics tools. This paper is part of his PhD thesis dissertation.

Author contributions: D.S., R.C., and D.J.H. conceived and designed the study and provided funding; D.S., G.S., V.L., and R.C. collected the samples; G.S., V.L., and D.S. generated the data; G.S., D.S., D.C., and P.C. analysed the data; D.S. and G.S. drafted the manuscript. All authors reviewed and approved the manuscript.

SUPPORTING INFORMATION

Additional supporting information may be found online in the Supporting Information section at the end of the article.

How to cite this article: Senczuk G, Harris DJ, Castiglia R, et al. Evolutionary and demographic correlates of Pleistocene coastline changes in the Sicilian wall lizard *Podarcis wagleriana*. *J Biogeogr*. 2018;00:1–14. https://doi.org/10.1111/jbi.13479